Structure and function of the catalytic site mutant Asp 99 Asn of phospholipase A₂: Absence of the conserved structural water

AMARENDRA KUMAR, CHANDRA SEKHARUDU, BOOPATHY RAMAKRISHNAN,
CYNTHIA M. DUPUREUR,[1] HONGXIN ZHU, MING-DAW TSAI,
AND MUTTAIYA SUNDARALINGAM

Departments of Chemistry and Biochemistry, The Ohio State University, Columbus, Ohio 43210

Abstract

To probe the role of the Asp-99···His-48 pair in phospholipase A₂ (PLA2) catalysis, the X-ray structure and kinetic characterization of the mutant Asp-99 → Asn-99 (D99N) of bovine pancreatic PLA2 was undertaken. Crystals of D99N belong to the trigonal space group P3₁21 and were isomorphous to the wild type (WT) (Noel JP et al., 1991, *Biochemistry 30*:11801–11811). The 1.9-Å X-ray structure of the mutant showed that the carbonyl group of Asn-99 side chain is hydrogen bonded to His-48 in the same way as that of Asp-99 in the WT, thus retaining the tautomeric form of His-48 and the function of the enzyme. The NH₂ group of Asn-99 points away from His-48. In contrast, in the D102N mutant of the protease enzyme trypsin, the NH₂ group of Asn-102 is hydrogen bonded to His-57 resulting in the inactive tautomeric form and hence the loss of enzymatic activity. Although the geometry of the catalytic triad in the PLA2 mutant remains the same as in the WT, we were surprised that the conserved structural water, linking the catalytic site with the ammonium group of Ala-1 of the interfacial site, was ejected by the proximity of the NH₂ group of Asn-99. The NH₂ group now forms a direct hydrogen bond with the carbonyl group of Ala-1.

Keywords: histidine tautomeric form; missing structural water; PLA2 D99N mutant; structure–function relationship; X-ray structure

Phospholipase A₂ (Fig. 1A) hydrolyzes the *sn*-2 ester bond of phospholipids. The studies on the mechanism of action of PLA2 have generated immense pharmacological interest. The mechanism involves binding of the enzyme to the lipid–water interface, productive binding of a single lipid molecule in the active site followed by hydrolysis (Scott et al., 1990). The interfacial binding site is essentially at the surface and includes the residues of the N-terminal helix-A, the calcium ion binding loop, and the loop connecting helix-D and the β-sheet (Dijkstra et al., 1981; see Kinemage 1). The c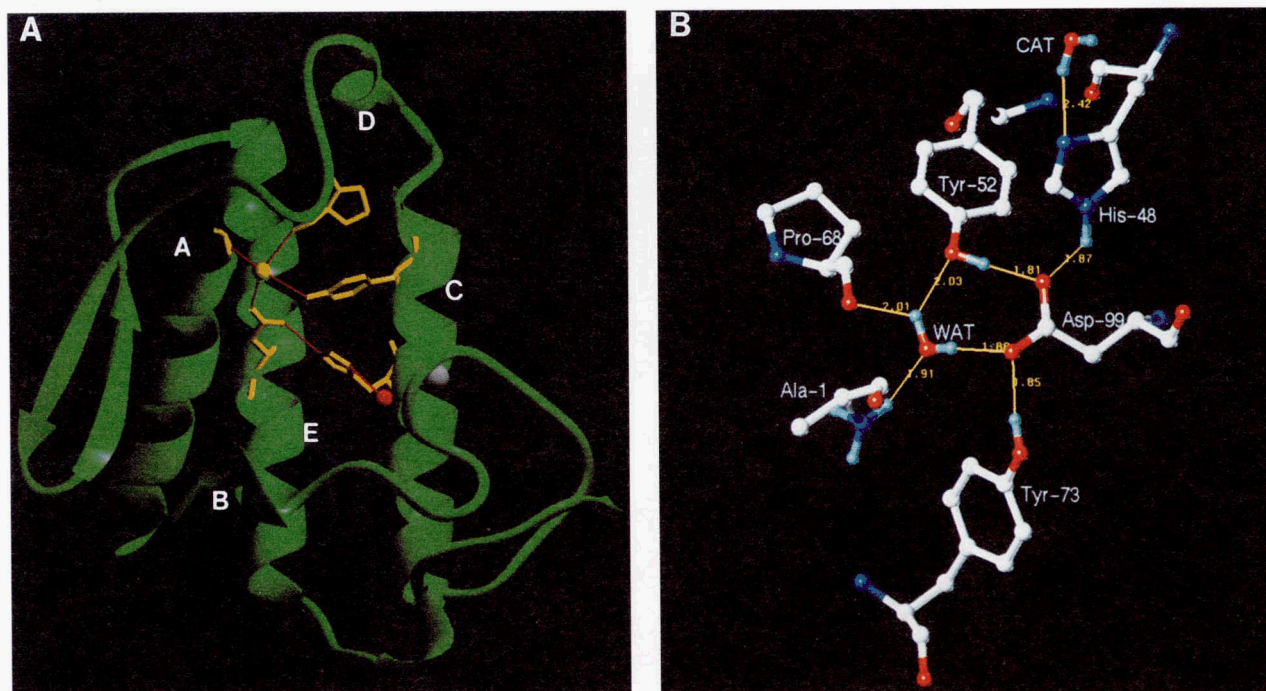atalytic triad Asp-99, His-48, and the water molecule is embedded between helices C and E. The structural water bridges the interfacial and the catalytic sites (Fig. 1A) and is conserved in all the known PLA2 structures. The hydrogen bonding network (Dijkstra et al., 1981; Noel et al., 1991) involving the structural water (Fig. 1B) is believed to lend structural support to the catalytic pocket (Brunie et al., 1985).

In trypsin, as in other serine proteases, the catalytic triad is composed of Asp, His, and Ser. The latter is replaced by a water molecule in PLA2. It was predicted that in trypsin, replacing the charged Asp residue by a neutral Asn would only reduce the rate of catalysis by a factor of 10 (Fersht, 1985). However, this was not the case for trypsin where there was a dramatic loss of catalytic activity by a factor of 10^4 (Craik et al., 1987) and the X-ray structure of the mutant D102N (Sprang et al., 1987) showed that the NH₂ group of Asn-102 side chain points toward His-57, resulting in the inactive tautomeric form. On the other hand, in the case of porcine pancreatic PLA2 mutant D99N, the loss in activity was only marginal and based on solution studies, it was suggested that the Asn-99 orients His-48 in the same way as Asp-99 in the WT (Kuipers et al., 1990). In

Fig. 1. A: Ribbon diagram (Carson, 1991) of WT phospholipase A_2 showing the structural water (yellow) and the hydrogen bonded residues Ala-1, Tyr-52, Pro-68, and Asp-99. The catalytic triad Asp-99, His-48, and the water (red) is also shown. The calcium ion is shown in gray. **B:** Hydrogen bonding scheme around the structural water molecule (WAT) in the WT PLA2. The catalytic water molecule is referred to as CAT.

order to probe this possibility we undertook X-ray structural and functional studies of bovine pancreatic PLA2. The X-ray structure of the mutant D99N shows that the Asn-99 side chain does have the same conformation as Asp-99 of the WT with the carbonyl oxygen pointing toward His-48 and retaining the correct tautomeric form. In addition, we were surprised to find from the X-ray structure that the conserved structural water molecule (Fig. 1B) was expelled and the NH_2 group of Asn-99 forms a direct hydrogen bond with the carbonyl group of Ala-1. These structural properties are used to explain the functional results (see Kinemage 1).

Results and discussion

The electron density was generally strong for the D99N mutant including the N-terminus, the catalytic site, and its surroundings, whereas for the loop regions 64–69 and 118–122 on the surface of the protein it was somewhat weaker. The electron density for the catalytic triad containing the mutated residue is shown in Figure 2. The RMS deviations in the bond distances (0.01 Å) and bond angles (2.8°) are comparable to those of the structures of the other PLA2 mutants determined in our laboratory. The RMS deviation for the $C\alpha$ atoms of the mutant from that of the WT (Noel et al., 1991) is 0.64 Å.

Two alternative orientations could be envisaged for the $CONH_2$ side chain of Asn-99 in the D99N mutant: (1) the NH_2 group of Asn-99 pointing toward His-48 and hydrogen bonding to it (Fig. 3A) and (2) the amino group pointing away and forming hydrogen bonds with the structural water and Tyr-73 (Fig. 3B). Both these schemes appear to involve only small

changes in orientation of the structural water and perturbations in the surrounding residues. We were therefore most surprised to find that the structural water was missing in the mutant (Fig. 3C; Kinemage 1), particularly when it was involved in 4
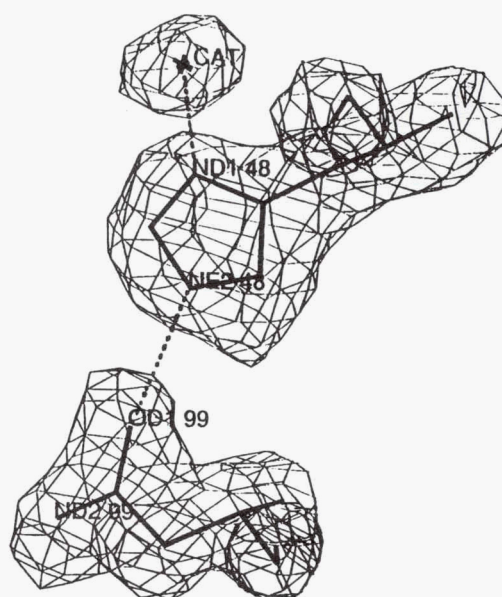

Fig. 2. A view of the Sim-weighted difference ($2F_o - F_c$) electron density map for the catalytic triad His-48, Asn-99, and catalytic water contoured at 1.2σ. The hydrogen bonds are shown by dashed lines.
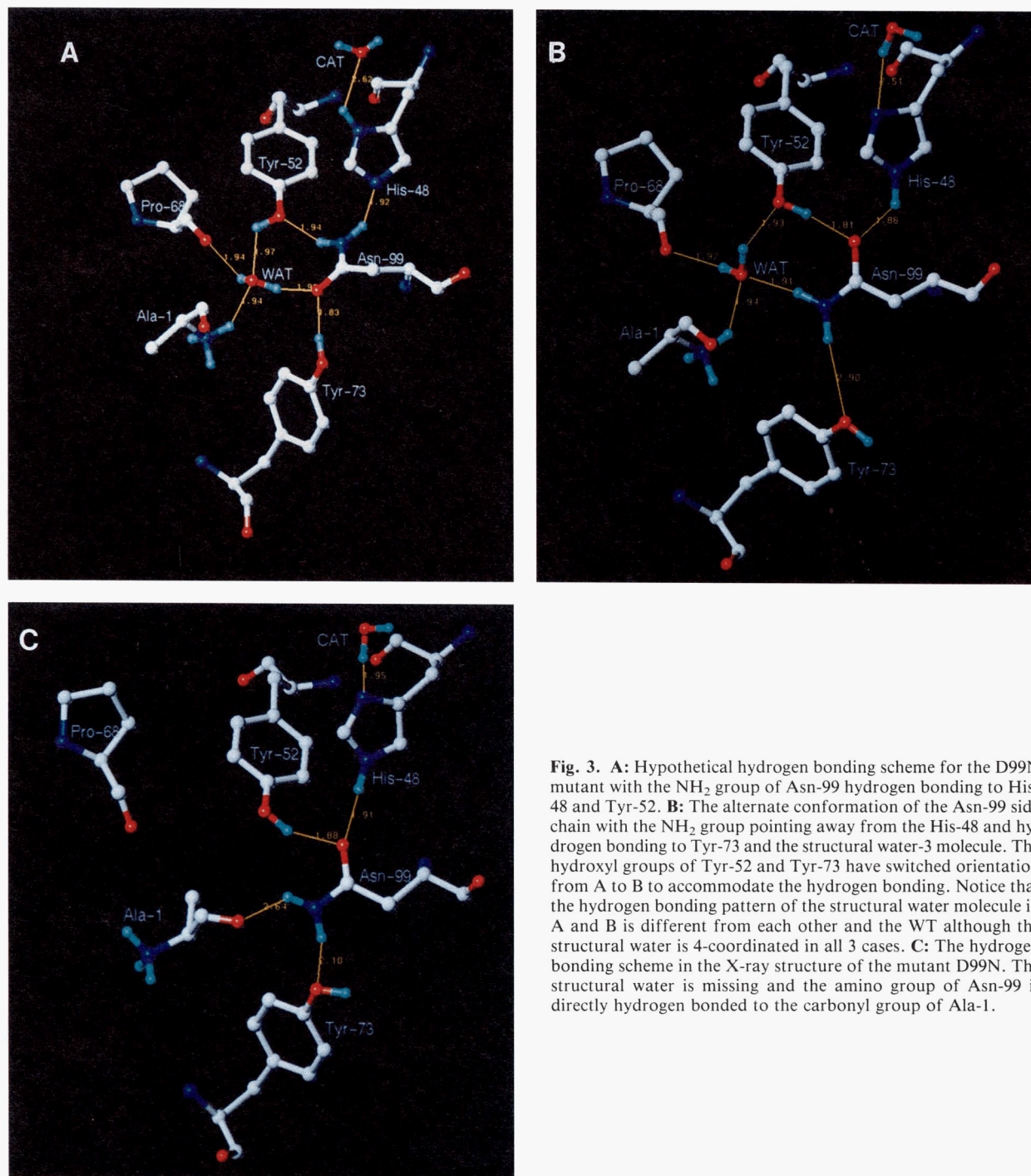
Fig. 3. A: Hypothetical hydrogen bonding scheme for the D99N mutant with the NH_2 group of Asn-99 hydrogen bonding to His-48 and Tyr-52. **B:** The alternate conformation of the Asn-99 side chain with the NH_2 group pointing away from the His-48 and hydrogen bonding to Tyr-73 and the structural water-3 molecule. The hydroxyl groups of Tyr-52 and Tyr-73 have switched orientation from A to B to accommodate the hydrogen bonding. Notice that the hydrogen bonding pattern of the structural water molecule in A and B is different from each other and the WT although the structural water is 4-coordinated in all 3 cases. **C:** The hydrogen bonding scheme in the X-ray structure of the mutant D99N. The structural water is missing and the amino group of Asn-99 is directly hydrogen bonded to the carbonyl group of Ala-1.

hydrogen bonds in the WT with Ala-1, Tyr-52, Pro-68, and Asp-99. The absence of the structural water results in a considerable rearrangement of the hydrogen bonding network. Ala-1 moves significantly (RMS of 1.38 Å from the WT) to form a direct hydrogen bond to NH_2 of Asn-99. Besides the movement, Ala-1 also undergoes a change in the backbone conformation ($\psi = 179°$ in WT $\rightarrow -39°$ in D99N), resulting in the NH_3^+ group pointing away from the catalytic triad. These changes re-

sult in Ala-1 partially filling the void created by the missing structural water molecule (Fig. 4A,B). In spite of these changes, the NH_3^+ group of Ala-1 retains 2 of its hydrogen bonds as in the WT, viz., to the $O\epsilon 1$ of Gln-4 and the carbonyl oxygen of Asn-71, whereas the third hydrogen bond to the structural water is now to the $O\delta 1$ of Asn-72 (Fig. 4C). Even though Ala-1 has moved considerably, its carbonyl group retains the α-helical hydrogen bond with the main-chain NH of Phe-5 as in the WT.
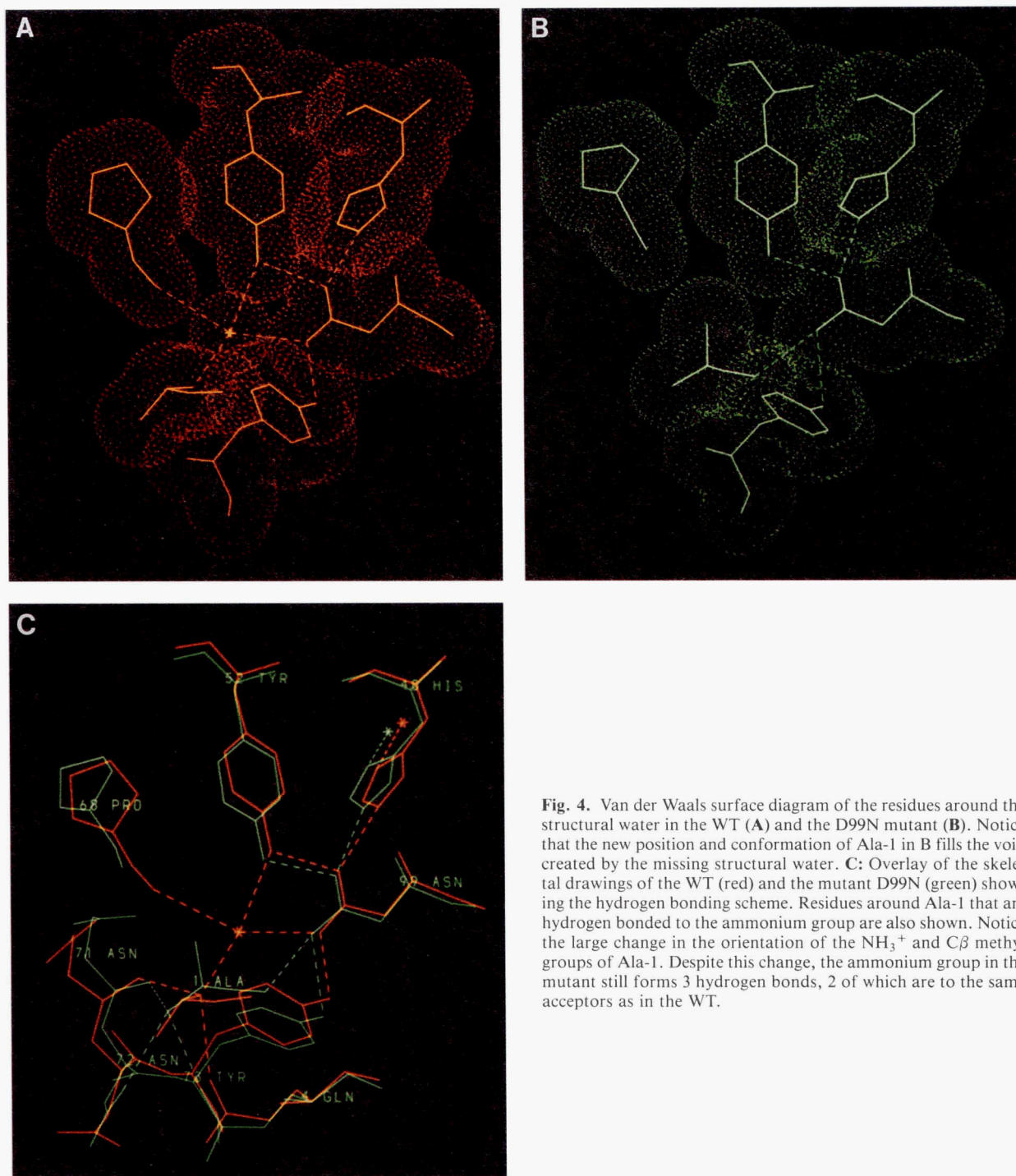
Fig. 4. Van der Waals surface diagram of the residues around the structural water in the WT (**A**) and the D99N mutant (**B**). Notice that the new position and conformation of Ala-1 in B fills the void created by the missing structural water. **C:** Overlay of the skeletal drawings of the WT (red) and the mutant D99N (green) showing the hydrogen bonding scheme. Residues around Ala-1 that are hydrogen bonded to the ammonium group are also shown. Notice the large change in the orientation of the NH_3^+ and $C\beta$ methyl groups of Ala-1. Despite this change, the ammonium group in the mutant still forms 3 hydrogen bonds, 2 of which are to the same acceptors as in the WT.

In the active site of the mutant there was a net loss of 3 hydrogen bonds: loss of 4 involved with the structural water and a gain of 1 from the Asn-99 to Ala-1.

Because the NH_2 group of the Asn-99 side chain is engaged in a direct *hand shake* with the carbonyl group of Ala-1, the C=O group points toward His-48, thus maintaining its tautomeric form as in the WT. Further, the hydrogen bonding between His-48 and the catalytic water of the triad has not changed from that of the WT. The alternate orientation of Asn-99 with NH_2 pointing toward His-48 is not feasible because of (1) the steric clash between the NH_2 group and the hydrogen atom on the $N\epsilon2$ of His-48 and (2) the repulsion between the carbonyl oxygen of the Asn-99 side chain and that of Ala-1.

Despite the conformational changes caused by the absence of the structural water the geometry of the catalytic triad (Fig. 2) has been little affected (RMS 0.25 Å). The $O\delta1(99)\cdots N\epsilon2(48)$

distance in the mutant (2.9 Å) is similar to that in the WT (2.8 Å). Further, the planes of the -$CONH_2$ group in D99N and COO^- group in WT are inclined at similar angles (39° versus 37°) to the plane of the imidazole ring of His-48. In the mutant, the catalytic water molecule deviates by 0.87 Å from the plane of the His-48 side chain and is at a distance of 2.8 Å from Nδ1. In the WT, the corresponding values are 0.92 Å and 3.2 Å, respectively. In both the structures, the catalytic water molecule is 4.1 Å away from the calcium ion. The side-chain conformation of Asn-99 in the mutant (χ1 = −66°, χ2 = 170°) and Asp-99 in the WT (χ1 = −75°, χ2 = 180°) are in the preferred (−)*gauche, trans* regions. His-48 also has the same conformation (χ1 = 180°, χ2 = −110°) in the mutant and the WT enzymes. All of these indicate that the tautomeric form of His-48 in D99N is the same as in the WT. On the contrary, in the D102N mutant of trypsin (Sprang et al., 1987) the Asn-102 side chain has switched so that the NH_2 group now points toward His-57. This changes the tautomeric form of His-57 and prevents it from abstracting a proton from Ser-195 and the enzymatic activity is lost.

The structural data can explain the relatively modest change in the kinetic constants of D99N compared to WT PLA2. As shown in Table 1, the k_{cat} of D99N decreases by 210-fold for DC_8PC micelles and 13-fold for DC_6PC monomers. Because the k_{cat} of micelles is only an apparent value, we further determined the v_0 and k_{cat} values at the surface of vesicles using scooting mode assays (Berg et al., 1991; Jain & Gelb, 1991). As shown in Table 1, the v_0 and k_{cat} values decrease by only 13-

Table 1. *Summary of properties of WT and D99N PLA2*

Parameters	WT	D99N
Conformational stability[a]		
$\delta G_d^{H_2O}$ (kcal/mol)	9.5	4.7
$D_{1/2}$ (M)	6.9	5.1
DC_8PC micelles		
$k_{cat,app}$ (s^{-1})	670	3.2
$K_{m,app}$ (mM)	1.4	2.0
DC_6PC monomers		
k_{cat} (s^{-1})	1.2	0.09
$DC_{14}PM$ vesicles[b]		
v_0 (s^{-1})	330	26
$N_s k_i$ (s^{-1})	30	9
k_{cat} (s^{-1})	670	35
K_M^*	0.65	0.25
k_{cat}/K_M^*	1,030	140
pH dependence[c]		
pH optimum	7.6	8.8
pK_{a1}	5.9	7.2
pK_{a2}	9.1	9.4

[a] Determined by guanidine-HCl-induced denaturation as reported (Pace, 1986). $\delta G_d^{H_2O}$ is the free energy of denaturation at zero concentration of guanidine-HCl, $D_{1/2}$ is the concentration at the midpoint, and *m* is a constant.

[b] See Berg et al. (1991) and Jain and Gelb (1991) for experimental procedures. Definition of kinetic parameters at the interface: K_M^*, Michaelis constant; k_{cat}, turnover number at saturating substrate concentration; $N_s k_i$, apparent second-order rate constant; v_0, turnover number when mole fraction of substrate = 1.

[c] Determined for the specific activity with 5 mM DC_8PC micelles.

and 20-fold, respectively. Other equilibrium dissociation constants at the interface do not vary greatly between WT and D99N. These results taken together suggest that the rate of the chemical step decreases by only ca. 20-fold for D99N PLA2, in contrast to the 10^4-fold decrease in the k_{cat} of D102N trypsin (Craik et al., 1987; Sprang et al., 1987).

The pH-rate profile was determined for both WT and D99N PLA2 in order to examine the effect of this mutation on the pK_a of His-48. The results are shown in Figure 5 and Table 1. The pK_{a1} and pK_{a2} of the WT (5.9 and 9.1, respectively) are in good agreement with the pK_a of His-48 (5.7) (Aguiar et al., 1979) and the pK_a of the amino-terminus (8.8) (Jansen, 1979), respectively, determined by NMR previously. Replacing the negatively charged Asp-99, which is expected to stabilize the protonated form of His-48, by a neutral Asn, one would predict the pK_a of His-48 to decrease. Consistent with this, the pK_{a1} of trypsin mutant D102N decreases by 1.5 pH units relative to WT trypsin (Craik et al., 1987). For the PLA2 mutant D99N, the increase in the pK_{a1} from 5.9 to 7.2 and in the pH optimum from 7.6 to 8.8 are contrary to expectations. The anomalous shift in the pK_{a1} of D99N PLA2 could be due to a number of factors, including the possibility that the pK_{a1} of the pH-rate profile of D99N PLA2 (Fig. 5) is not a true reflection of the pK_{a1} of His-48. This possibility was further examined by directly determining the pK_a of His-48 from NMR.

In the WT enzyme, the H_2 of His-48 displays a pK_a of 5.7 (Aguiar et al., 1979). In D99N, a distinct resonance, possibly arising from the H_2 of the His-48, does not display a clear chemical-shift change from pH 8.9 (8.463 ppm) to 4.7 (8.462 ppm). The pK_a apparently has been shifted to less than 4.7 because, below this pH, the peak is broadened and shifted to 8.28 ppm at pH 2.6; however, the exact pK_a cannot be determined because the enzyme appears to undergo denaturation at this low pH range. Thus the NMR analysis suggests that in PLA2, the pK_a of His-48 decreases from the WT to D99N by more than 1.0 pH unit as
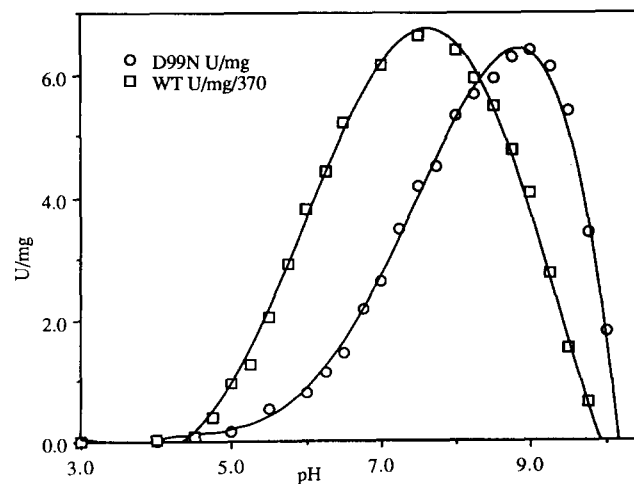
Fig. 5. The pH profiles of WT and D99N PLA2 activities toward DC_8PC micelles, determined with saturating substrate (5 mM) at 45 °C in 1 mM sodium borate, 25 mM $CaCl_2$, 100 mM NaCl, and 0.1 mM EDTA. Notice that the vertical scale of the WT has been scaled down by a factor of 370. A pH point at each side of the curve has been selected to verify that $K_{m,app}$ does not change significantly from the value reported in Table 1.

expected. The anomalously high pK_{a1} of D99N obtained from the pH–rate profile could be caused by other factors contributing to the catalysis. Further investigation will be required to firmly establish the reason for the anomaly.

Because in the WT PLA2 the structural water connects the catalytic site residues with those of the interfacial site, we also examined whether interfacial site residues and interfacial binding have been perturbed in D99N. Ala-1, an important residue for interfacial catalysis (Dijkstra et al., 1984), has indeed moved considerably and also changed its conformation. Leu-19, another important residue in the interfacial binding site (Dijkstra et al., 1981) or in the hydrophobic channel (White et al., 1990), has also undergone a large conformational change from a type-II reverse turn (comprised of residues 17–20) to a type-III ($\psi = +38°$ in the WT and $\psi = -25°$ in the mutant) (Fig. 6). These conformational changes have not affected the binding of the enzyme to the interface. There is no evidence from the fluorescence binding studies (Jain & Maliwal, 1993) of any substantial change in the substrate binding of the enzyme to the interface (M.K. Jain, unpubl. results). This shows that the modest decrease in catalysis, comparable to that observed for the Asn-mutant of porcine pancreatic PLA2 (Kuipers et al., 1990), probably arises due to a perturbation in the hydrolysis step rather than interfacial binding.

This is the first X-ray structural evidence which shows that Asn-99 of the mutant D99N orients His-48 in the same way as Asp-99 in the WT (see Kinemage 1). An unexpected result from the study is that the structural water molecule is eliminated in order to allow the NH₂ group of Asn-99 to point away from
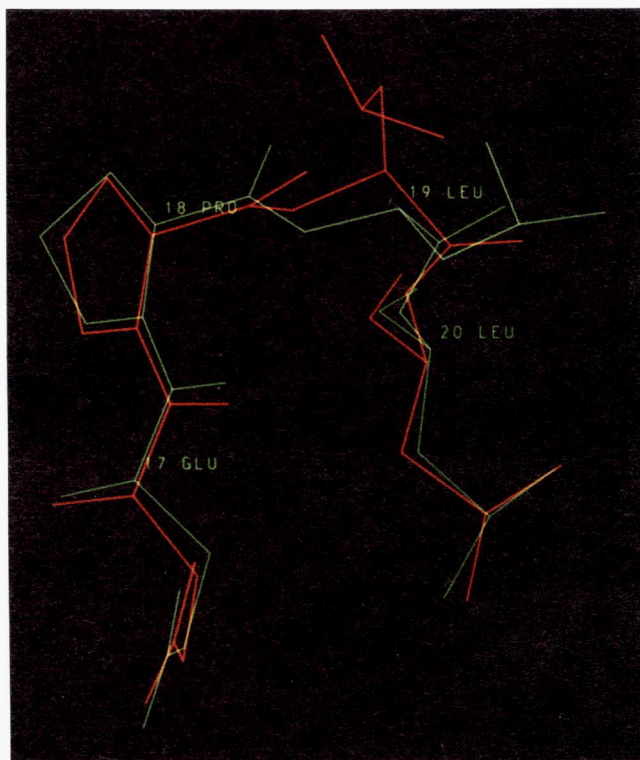
His-48. This preserves the hydrogen bonding pattern of the catalytic triad and the tautomeric form of His-48 as in the WT and hence the enzyme remains functional. It was believed that the precise architecture at the N-terminal end is crucial in the interfacial binding (Slotboom et al., 1977; Dijkstra et al., 1984). The present work indicates that although the enzyme loses its structural water, it can adapt itself by redistributing the hydrogen bonding network at the N-terminus and undergo some conformational changes to retain its micelle binding. The absence of the structural water molecule affects the surrounding structure, which can possibly explain the reported increase in the flexibility and the decrease in the stability of D99N (Dupureur et al., 1992).

Materials and methods

The kinetic methods used in this work were carried out according to the reported procedures (Berg et al., 1991; Jain & Gelb, 1991; Noel et al., 1991; see also Table 1). The crystals of the D99N mutant of the recombinant bovine pancreatic PLA2 were grown using the conditions described earlier (Noel et al., 1991). The crystals belong to the trigonal system, space group P3₁21, cell dimensions, $a = b = 46.11$, and $c = 102.10$ Å. The intensity data out to 1.9 Å were collected, at room temperature, on our in-house Siemens area detector using a Max Science rotating anode source operating at 50 kV and 90 mA. The crystal-to-detector distance was 12.5 cm and the exposure time was 90 s per frame. The data were obtained from a $0 \rightarrow 180°$ ϕ scan and 3 ω scans at different ϕ and χ values with an increment of 0.2°. In all, 10,307 unique reflections $[F > 1\sigma(F)]$ were collected with an R_{sym} of 0.06. The intensity data were reduced using the XENGEN-2.0 software package (Howard, 1990). Because the mutant crystal was isomorphous to that of the WT (P3₁21, cell dimensions $a = b = 46.52$, and $c = 102.20$ Å) its coordinates formed the starting model for the refinement. The structure was refined using X-PLOR 3.0 (Brünger, 1992). The protein was fitted to the Sim-weighted difference-electron density maps using the program package FRODO 6.6 (Jones, 1985) on our Evans and Sutherland molecular graphics system ESV30. The refinement dropped the R-value to 21.5%. At this point water molecules were included in the refinement. In all, 81 water molecules were located from the difference map by applying the same criteria as before (Sekharudu et al., 1992). Refinement of the structure including the water molecules gave a final R-value of 18.5% for the 8,870 reflections $[F > 3\sigma(F)]$ in the resolution range 6.5–1.9 Å. The final model was comprised of 957 protein atoms, 1 calcium ion, and 81 water molecules. The average error in the atomic coordinates estimated from Luzzati plots (Luzzati, 1952) is about 0.2 Å. The atomic coordinates have been deposited in the Brookhaven Protein Data Bank (reference 1CEH).

Fig. 6. The switch from the type-II reverse turn in the WT (red) to the type-III in the D99N mutant (green) involving residues 17–20.

References

Aguiar A, de Haas GH, Jansen EHJM, Slotboom AJ, Williams R. 1979. Proton nuclear magnetic resonance/pH titration studies of the histidines of pancreatic phospholipase A_2. *Eur J Biochem 100*:511-518.

Berg OG, Yu BZ, Gogers J, Jain MK. 1991. Interfacial catalysis by phospholipase A_2: Determination of the kinetic rate constants. *Biochemistry 30*:7283-7297.

Brünger AT. 1992. *X-PLOR manual*. New Haven, Connecticut: Yale University.

Brunie S, Brolin SJ, Gerwirth D, Sigler PB. 1985. The refined crystal structure of dimeric phospholipase A_2 at 2.5 Å: Access to a shielded catalytic center. *J Biol Chem 260*:9742-9749.

Carson M. 1991. *Ribbons 2.0 manual*. Birmingham: University of Alabama.

Craik CS, Roczniak S, Largman C, Rutter WJ. 1987. The catalytic role of the active site aspartic acid in serine proteses. *Science 237*:909-913.

Dijkstra BW, Drenth J, Kalk KH. 1981. Active site and catalytic mechanism of phospholipase A_2. *Nature 289*:604-606.

Dijkstra BW, Kalk BW, Drenth J, de Haas GH, Egmond MR, Slotboom AJ. 1984. Role of the N-terminus in the interaction of pancreatic phospholipase A_2 with aggregated substrates. Properties and crystal structure of transaminated phospholipase A_2. *Biochemistry 23*:2759-2766.

Dupureur CM, Li Y, Tsai MD. 1992. Phospholipase A_2 engineering 6: Single amino acid substitutions of active site residues convert the rigid enzyme to highly flexible conformational states. *J Am Chem Soc 114*:2748-2749.

Fersht A. 1985. *Enzyme structure and mechanism*. New York: Freeman. pp 405-413.

Howard AJ. 1990. *A guide to macromolecular X-ray data reduction for the Siemens area detector system. The XENGEN system, version 2.0.* Gaithersburg, Maryland: Genex Corporation.

Jain MK, Gelb MH. 1991. Phospholipase A_2-catalyzed hydrolysis of vesicles: Uses of interfacial catalysis in the scooting mode. *Methods Enzymol 197*:112-125.

Jain MK, Maliwal BP. 1993. Spectroscopic properties of the states of pig pancreatic phospholipase A_2 at interfaces and their possible molecular origin. *Biochemistry 32*:11838-11846.

Jansen EHJM. 1979. NMR studies on pancreatic phospholipase A_2 [thesis]. Utrecht, The Netherlands: State University of Utrecht.

Jones TA. 1985. Interactive computer graphics: FRODO. *Methods Enzymol 115*:157-171.

Kuipers OP, Franken PA, Hendriks R, Verheij HM, de Haas GH. 1990. Function of fully conserved residues Asp 99, Tyr 52 and Tyr 73 in phospholipase A_2. *Protein Eng 4*:199-204.

Li Y, Tsai MD. 1993. Phospholipase A_2 engineering. 10. The aspartate··· histidine catalytic diad also plays an important structural role. *J Am Chem Soc 115*:8523-8526.

Luzzati V. 1952. Traitement statistique des erreurs dans la determination des structures cristallines. *Acta Crystallogr 5*:802-807.

Noel JP, Bingman CA, Deng T, Dupureur CM, Hamilton KJ, Jiang RT, Kwak JG, Sekharudu C, Sundaralingam M, Tsai MD. 1991. Phospholipase A_2 engineering: X-ray structural and functional evidence for the interaction of lysine-56 with substrates. *Biochemistry 30*:11801-11811.

Pace CN. 1986. Determination and analysis of urea and guanidine hydrochloride denaturation curves. *Methods Enzymol 131*:266-280.

Scott DL, White SP, Otwinowski Z, Yuan W, Gelb MH, Sigler PB. 1990. Interfacial catalysis: The mechanism of phospholipase A_2. *Science 250*:1541-1546.

Sekharudu C, Ramakrishnan B, Huang B, Jiang RT, Dupureur CM, Tsai MD, Sundaralingam M. 1992. Crystal structure of the Y52F/Y73F double mutant of phospholipase A_2: Increased hydrophobic interactions of the phenyl groups compensate for the disrupted hydrogen bonds of the tyrosines. *Protein Sci 1*:1585-1594.

Slotboom AJ, van Dam-Mieras MCE, de Haas GH. 1977. Regulation of phospholipase A_2 activity by different lipid-water interfaces. *J Biol Chem 252*:2948-2951.

Sprang S, Standing T, Fletterick RJ, Stroud RM, Finer-Moore J, Xuong NH, Hamlin R, Rutter WJ, Craik CS. 1987. The three-dimensional structure of Asn[102] mutant of trypsin: Role of Asp[102] in serine protease catalysis. *Science 237*:905-909.

White SP, Scott DL, Otwinowski Z, Gelb MH, Sigler PB. 1990. Crystal structure of cobra-venom phospholipase A_2 in a complex with a transition state analogue. *Science 250*:1560-1563.